



Published in final edited form as:

J Biomed Mater Res A. 2018 July ; 106(7): 2048–2058. doi:10.1002/jbm.a.36400.

Self-assembled, Ellipsoidal Polymeric Nanoparticles for Intracellular Delivery of Therapeutics

Prachi Desai¹, Anjana Venkataramanan¹, Rebecca Schneider^{2,3}, Manish K. Jaiswal¹, James K. Carrow¹, Alberto Purwada^{2,4}, Ankur Singh^{2,4,*}, and Akhilesh K. Gaharwar^{1,5,6,*}

¹Department of Biomedical Engineering, Texas A&M University, College Station, TX 77843 (USA)

²Sibley School of Mechanical and Aerospace Engineering, Cornell University, Ithaca, NY 14853 (USA)

³Robert Frederick Smith School of Chemical and Biomolecular Engineering, Cornell University, Ithaca, NY 14853

⁴Meinig School of Biomedical Engineering, Cornell University, Ithaca, NY 14853 (USA)

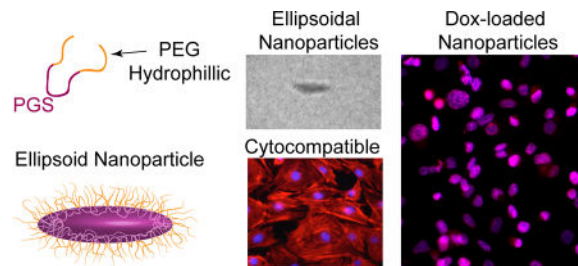
⁵Department of Materials Science and Engineering, Texas A&M University, College Station, TX 77843 (USA)

⁶Center for Remote Health Technologies and Systems, Texas A&M University, College Station, TX 77843 (USA)

Abstract

Nanoparticle shape has emerged as a key regulator of nanoparticle transport across physiological barriers, intracellular uptake and biodistribution. We report a facile approach to synthesize ellipsoidal nanoparticles *via* self-assembly of poly(glycerol sebacate)-co-poly(ethylene glycol) (PGS-*co*-PEG). The PGS- PEG nanoparticle system is highly tunable, and the semi-axis length of the nanoparticles can be modulated by changing PGS-PEG molar ratio and incorporating therapeutics. As both PGS and PEG are highly biocompatible, the PGS-*co*-PEG nanoparticles show high hemo-, immuno- and cyto- compatibility. Our data suggest that PGS-*co*- PEG nanoparticles have the potential for use in a wide range of biomedical applications including regenerative medicine, stem cell engineering, immune modulation and cancer therapeutics.

Graphical abstract



* Corresponding authors: gaharwar@tamu.edu (A.K.G); as2833@cornell.edu (A.S).

Keywords

Shape-specific nanoparticles; drug delivery; therapeutic delivery; bovine serum albumin

1. Introduction

Nanoengineered particles have been extensively investigated for delivery of therapeutics to cells and tissues for regenerative medicine, stem cell engineering, immune modulation, and cancer therapeutics.¹⁻⁴ By modulating the physiochemical characteristics of nanoparticles, therapeutic efficacy, cellular internalization, biodistribution and *in vivo* retention can be customized.⁵⁻⁹ For example, the size of these nanoparticles regulates their own uptake by the healthy (stem cells) or diseased cells (such as tumors or immune cells).¹⁰⁻¹⁴ Smaller nanoparticles (~25 nm) are preferentially transported through the lymphatics drainage system to draining lymph nodes compared to larger (~100 nm) nanoparticles.¹⁵ Smaller spherical nanoparticles are effective in delivering cargo within the cellular structures as they are readily endocytosed by cells compared to larger size nanoparticles. Whereas, for extracellular delivery and prolonged retention of therapeutics, larger sized nanoparticles have been shown to higher efficacy compared to smaller size nanoparticles.^{5-8,10}

Recently, along with the size, the shape of the nanoparticles has also emerged as a key regulator of intracellular delivery and therapeutic transport efficacy across physiological barriers.¹⁶⁻¹⁹ In addition, non-spherical nanoparticles have been shown to respond differently to endocytosis, intracellular retention, and *in vivo* circulation time. For example, elongated nanoparticles show a superior pharmacokinetics profile and reduced non-specific cellular uptake compared to spherical nanoparticles.^{18,20,21} In addition, non-spherical nanoparticles have shown to respond differently to endocytosis, intracellular retention, and *in vivo* circulation time. For example, elongated nanoparticles showed a superior pharmacokinetics profile and reduced non-specific cellular uptake compared to spherical nanoparticles.²² Thus, there is extensive interest in investigating the potential of non-spherical nanoparticles for therapeutic delivery.

Non-spherical nanoparticles, such as nanorods and nanodiscs, are effectively taken up by cells compared to their spherical counterpart.²³⁻²⁷ The exact mechanism responsible for preferential internalization of non-spherical particles compared to spherical particles is not well understood. However, increasing the surface area of rod- and disc-shaped nanoparticles as compared to spherical nanoparticles is believed to play an important role during cellular internalization.²³⁻²⁷ Nanoparticles with large surface-contact area results in stronger adhesion force and thus promote faster cellular uptake, compared to particles with small surface-contact area. Internalization of nanoparticles is attributed to complex interplay between the surface area in contact with the cell membranes and strain energy required for membrane deformation.²³⁻²⁷

The majority of recent studies in this area have focused on non-spherical shapes such as rods and discs^{6,19,21}; however, little information exists on the role of ellipsoidal-shaped nanoparticles. Similar to rod-shaped nanoparticles, ellipsoidal nanoparticles also have higher surface-to-volume ratio compared to spherical nanoparticles.²⁸ Due to absence of any sharp

edges in ellipsoidal nanoparticles, surface strain required by cell membrane will be lower compared to rod-shaped nanoparticles. Accordingly, ellipsoidal nanoparticles for therapeutic delivery need further study. However, due to the lack of suitable polymers, it is difficult to fabricate ellipsoidal nanoparticles using conventional techniques such as self-assembly, flash nanoprecipitation and microfluidics-based preparation.^{28–31}

Here, we report synthesis of self-assembled ellipsoidal nanoparticles from copolymer consisting of poly(glycerol sebacate) (PGS) and poly(ethylene glycol) (PEG). PGS is biocompatible elastomeric polyester extensively investigated for soft tissue replacement and regeneration.^{32–34} The degradation products of PGS, glycerol and sebacic acid are endogenous constituents and thus readily metabolize under physiological conditions.^{32,33} Due to the elastomeric properties and biocompatibility, PGS-based scaffolds have been investigated for cartilage regeneration, cardiac patches, bone scaffolds, and nerve conduits.³⁵ Despite these advantages, to our knowledge ellipsoidal-shaped nanoparticles of PGS or copolymers of PGS have not been developed.

Earlier studies have highlighted the role of surface properties in controlling cellular internalization and therapeutic efficacy.^{36,37} Due to high surface energy of nanoparticle surface, proteins from biological media form protein corona that dictate cellular fate of nanoparticles. PEGylating of polymeric particles results in limited non-specific physical interactions and enhances nanoparticle stability.^{38,39} It is our expectation, that PEGylating of PGS can improve hydrophilicity, increases stability in serum, and prolong circulation. We synthesized PGS-*co*-PEG copolymer with different PGS:PEG molar ratio. Nanoparticles from PGS-*co*-PEG polymers will be synthesized *via* the nanoprecipitation method. PEGylation of PGS, results in formation of a core-shell nanoparticles with PGS core and PEG shell. We will investigate the hemo-, immune- and cyto- compatibility of PGS-PEG nanoparticles. Our report introduces a new family of ellipsoidal PGS-PEG nanoparticles for intercellular delivery and can be used to deliver a range of biomolecules for biomedical applications.

2. Experimental

Synthesis of copolymer

PGS-*co*-PEG polymers were synthesized by two-step polycondensation reaction with two different molar ratios of PEG segment (20 and 40) within the copolymer system using previously reported method.⁴⁰ The first step involved the polycondensation of sebacic acid (20.22 gm) and poly (ethylene glycol) (20 or 40 gm) in 250mL three neck flask under stirring conditions. PEG was dried in vacuum chamber at 90°C before its use. The reaction was carried out further at 130°C under the flow of argon for 2h and under vacuum of 50mTorr for another 24h. In the second step a specific amount of glycerol (7.368 gm) was added, mixed thoroughly under the flow of argon and the reaction was carried out at 130°C under reduced pressure of 50mTorr for another 48h.⁴⁰ Gel permeation chromatography (GPC, Waters, Milford, MA) was used to determine the molecular weight of copolymers using tetrahydrofuran (THF) as solvent. The overall diol to dicarboxylic acid molar ratio was kept constant. Two molar ratios of PEG to glycerol (20/80, and 40/60) were used to develop PGS-*co*-PEG polymers with different degrees of PEG segments within the resulting

copolymer system. A close control over the condensation reaction resulted in narrow polydispersity index (PDI) for PGS-20PEG ($M_w \sim 4998$ Da, PDI=1.48) and PGS-40PEG ($M_w \sim 4037$ Da, PDI=1.42).

Synthesis of nanoparticle

Nanoprecipitation method is extensively used to synthesize polymeric nanoparticles and to entrap hydrophilic drugs or proteins.^{41,42} Here, we have prepared PGS-*co*-PEG nanoparticles *via* the nanoprecipitation method (Fig 1a). Briefly, 5% (w/v) of the polymer was dissolved in DMSO and was slowly added drop wise to an aqueous phase to obtain self-assembled nanoparticles. The resulting solution was homogenized using a bath sonicator. Finally, the nanoparticles were collected at 17,000 rpm (20 minutes) using Beckman Optima™ MAX-XP tabletop ultracentrifuge fitted with TLA-55 Rotor and washed thrice. Later precipitated nanoparticle was suspended in 10mL PBS to obtain nanoparticle solution (5 mg/mL).

Therapeutic Encapsulation

Fluorescein isothiocyanate-labeled bovine serum albumin (FITC-BSA) was encapsulated within PGS-*co*-PEG nanoparticles during nanoprecipitation method. 0.5% of FITC-BSA was added to aqueous phase prior to addition of 5% (w/v) of the polymer dissolved in DMSO. During nanoparticle formation, FITC-BSA was entrapped within the nanoparticles. The amount of FITC-BSA remaining in supernatant after nanoparticle formation was determined using UV/Vis spectroscopy (n=3). Encapsulation efficiency (EE%) was determined by Eq. 1:

$$EE(\%) = \frac{FITC-BSA(initial) - FITC-BSA(supernatant)}{FITC-BSA(initial)} \times 100\% \quad \text{Eq. 1}$$

FITC-BSA (initial) = total amount of FITC-BSA added initially; and FITC-BSA (supernatant) = amount of FITC-BSA in the supernatant measured by quantitative UV/Vis spectroscopy.

Physicochemical characterization of nanoparticles

The mean particle size (hydrodynamic diameter), and electrophoretic mobility of PGS-*co*-PEG nanoparticles were determined using dynamic light scattering (DLS) (Malvern Instrument, UK) (n=3). The electrophoretic mobility of the co-polymers was also measured using DLS (n=3). The stability of nanoparticles under physiological conditions (in PBS and T=37°C) was monitored for three weeks. The morphological characterization of the nanoparticles was performed using JEOL JEM-2010 transmission electron microscopy (TEM) by loading nanoparticle suspension on lacey carbon grid. The sizes of the nanoparticles were quantified using ImageJ (NIH) by counting >250 particles from TEM images to determine length and width of the nanoparticles.

Cellular characterization of PGS-co-PEG nanoparticles

Preosteoblast cell lines (NIH MC3T3 E1–4, ATCC, USA) were used to determine the cytotoxicity of nanoparticles (n=5). Cells were seeded in a 48-well flat-bottomed plate at a density of 1.5×10^4 cells/well in normal growth media (Alpha MEM, supplemented with 10% FBS and 1% penicillin/streptomycin (100 U/100 µg/ml); Life Technologies, USA) and were allowed to adhere for 1 day. After 1 day, cells were treated with PGS-co-PEG at different concentrations (0.15, 0.3, 0.6, 1.25, 2.5, 5, 10 mg/mL). After incubating for 3 h and 24 h, the cells were washed with PBS (2×) and fixed with glutaraldehyde solution (2%) for 10–15 minutes. The fixed cells were stained with rhodamine-labeled phalloidin (R415, Life Technology, USA) and counter stained with 4'6-diamidino-2-phenylindole dilactate (DAPI). The cells were imaged using fluorescence microscope (TE a2000-S, Nikon, USA). Nanoparticles cytotoxicity was determined using the MTS assay (3-(4,5-dimethylthiazol-2-yl)-5-(3-carboxymethoxyphenyl)-2-(4-sulfophenyl)-2H-tetrazolium) according to the manufacturer's protocol.

Hemocompatibility of nanoparticles

The hemolytic ability of our nanoparticles was investigated using a previously reported method⁴³ using fresh bovine blood obtained from Texas A&M College of Veterinary Medicine & Biomedical Sciences, College Station, TX (n=3). Briefly, Red blood cells (RBCs) were separated from whole blood by centrifugation (2800rpm, 15 minutes, 5 cycles). The purified RBCs were diluted with PBS to obtain working solution. Nanoparticles with varying concentration (A_{NP}) was added to RBC solution (1 mL) or whole blood (1 mL) and incubated for 3 h at 37°C (n=5). RBCs incubated with water (A_W) were used as positive control and RBCs incubated with PBS alone (A_{PBS}) was used as negative control. After the incubation time, the solution was centrifuged at 2000g for 6 minutes and supernatant (10 µl) was added to Drabkin's reagent (100 µl) for quantitative calorimetric determination of hemoglobin concentration. The absorbance was read at 540 nm using a microplate reader (Infinite M200 PRO, TECAN). Hemolysis was determined by absorbance using equation: Hemolysis (%) = $((A_{NP} - A_{PBS}) / (A_W - A_{PBS})) * 100$

Cellular internalization

To investigate the endocytosis pathway, we looked into three different pathways namely micropinocytosis, calveolae mediated endocytosis and clathrin mediated endocytosis pathways (n=3). We investigate three different endocytosis pathways – i.e., (i) micropinocytosis, (ii) calveolae-mediated and (iii) clathrin-mediated – using the inhibitor drugs Wortmannin (400 nM), Nystatin (10 µM) and Chlorpromazine (35 µM) to block the respective pathways. First, cells were treated with these inhibitory drug at 37 °C for 30 mins. Then, cells are subjected to PGS-40PEG nanoparticles for 3 hours. After 3 hours of incubation, the cells were washed thoroughly with PBS and they were trypsinized to perform flow cytometry using BD Accuri™ C6 Cytometer - BD Biosciences. The cellular uptake was investigated using two different cell lines pre-osteoblasts (NIH MC3T3 E1–4, ATCC, USA) and endothelial cells (HUVEC, C2519A, Lonza Inc) lines.

Immunocompatibility of nanoparticles

Macrophage activation studies were performed by seeding 20,000 RAW 264.7 murine macrophage cell line (ATCC) in a 24-well plate (n=3). Following 24 h of incubation, nanoparticles were reconstituted in PBS and introduced to the cells at two different doses: 10 and 100 $\mu\text{g}/\text{mL}$. Analysis on macrophage activation was carried out after 48 h of incubation using flow cytometry with antibodies (eBioscience) targeted against two macrophage activation cell surface markers: CD80 and CD86.

Statistical analysis

The data was presented as mean \pm standard deviation (n=3–5). Statistical analysis was performed using a one-way analysis of variance (ANOVA) with Turkey's post hoc test for pairwise comparison. Statistical significance is designated with *via* an asterisk * $p < 0.05$.

3. Results and discussion

3.1 Synthesis and Characterization of Ellipsoidal Nanoparticles

Nanoparticles from PGS-*co*-PEG polymers were synthesized *via* the nanoprecipitation method (Fig 1a). Briefly, copolymer was dissolved in DMSO and added to phosphate buffer saline (PBS) in a drop-wise manner to obtain self-assembled nanoparticles. This technique was based on dissolving the polymer in a water-miscible solvent followed by drop wise addition to an excess volume of aqueous phase with continual stirring. The nanoparticles were formed and precipitated during the solvent evaporation.

We hypothesized that PGS-PEG nanoparticles were formed due to the self-assembly by noncovalent interactions, which results in formation of highly organized supramolecular systems. PGS-*co*-PEG is an amphiphilic copolymer composed of hydrophobic PGS and hydrophilic PEG blocks with different polarities. PGS-*co*-PEG is completely dissolved in DMSO, but in aqueous solution they form supramolecular assemblies due to thermodynamic incompatibility between PGS and PEG blocks. It is expected that the interfacial tension between the PGS-*co*-PEG and the solvent mixture might result in the formation of PGS-PEG nanoparticles. When we prepared nanoparticles using PGS alone, nanoparticles were forming but started aggregating in few minutes and settle down. A plausible reason for this observation could be the hydrophobic nature of PGS. It might be possible that by modulating the molecular weight or type of solvent used, it is possible to obtain stable PGS nanoparticles. In current study, we modified PGS with PEG to increase the hydrophilicity and to provide stability to the nanoparticles.

To confirm the presence of PEG on the surface of nanoparticles, we determined the electrophoretic mobility of copolymer and nanoparticles. Both PGS-20PEG and PGS-40PEG copolymers had similar zeta potentials of -38.3 ± 4.3 mV and -39.5 ± 4.1 mV respectively, due to the presence of hydroxyl groups on the PGS backbone (Fig 1b). After nanoparticle formation, the zeta potentials were decreased to -21.3 ± 3.9 mV and -23.7 ± 3.5 mV for PGS-20PEG and PGS-40PEG, respectively. The decrease in zeta potential suggests that PGS formed the core of the nanoparticles and PEG shielded the surface of the nanoparticles to provide aqueous stability. Other studies have shown the formation of core-

shell nanoparticles from copolymer systems such as poly(lactic-co-glycolic acid) (PLGA)-*co*-PEG⁴⁴, poly (d, l-lactic acid)(PLA)-*co*-PEG⁴⁵ and poly(caprolacton)(PCL)-*co*-PEG⁴⁶. In addition, nanoparticles containing PEG chains on their surface have ability to provide stealth characteristics⁴⁷ and thus can be used for systemic drug administration.³⁷

3.2 Morphology of Self-assembled Nanoparticles

To determine the morphology of self-assembled nanoparticles, transmission electron microscopy (TEM) and dynamic light scattering (DLS) were used. TEM indicated formation of elongated ellipsoidal nanoparticles from PGS-20PEG and PGS-40PEG (Fig. 1c).

Quantification of images using IMAGE J (NIH) determined that PGS-20PEG nanoparticles were $\sim 235 \pm 132$ nm in length and $\sim 48 \pm 28$ nm in width and PGS-40PEG nanoparticles were $\sim 195 \pm 110$ nm in length and $\sim 80 \pm 48$ nm in width (Fig. 1c). The hydrodynamic diameter (D_h) of the PGS-PEG nanoparticles as determined by DLS also correlates with the data obtained from TEM. PGS-20PEG nanoparticles were $D_h \sim 311$ nm and PGS-40PEG nanoparticles were $D_h \sim 250$ nm. The increase in PEG concentration from PGS-20PEG to PGS-40PEG resulted in reduction in D_h due to enhanced stability provided by PEG chains. It is expected that increase in PEG concentration, imparts higher aqueous stability to PGS-40PEG compared to PGS-20PEG. Earlier studies have shown that by modulating the ratio between copolymer chains, it is possible to change the size and shape of nanoparticles.^{19,48} Our current study extends the concept of modulating the size of nanoparticle by changing co-polymer ratio towards elliptical nanoparticles. Earlier studies have shown that ellipsoidal nanoparticles are highly relevant to physical and biochemical targeting *via* both systemic and site-specific deliveries.²⁹ This is due to enhanced interfacial surface between nanoparticles and cell membrane.

From TEM and DLS studies, it is observed that we can modulate the size of elliptical nanoparticles by controlling the molar ratio between PGS and PEG. We hypothesize that the elliptical nanoparticles are formed due to block characteristics of PGS-PEG copolymer and thermodynamic incompatibility between different blocks. By modulating the ratio between PGS and PEG in the copolymer system, we can change the hydrodynamic volume fraction of PGS block with respect to the PEG block. The ratio between PGS and PEG block was also shown to dictate size of major and minor axis in the elliptical nanoparticles.

3.3 Modulating Size of Nanoparticle via Therapeutic Loading

The size of nanoparticles has shown to play an important role in cellular internalization, tissue localization and biodistribution.^{49,50} The nanoprecipitation technique can be used to encapsulate a range of hydrophilic drugs and protein within nanoparticle.^{41,42} To evaluate the feasibility of loading a therapeutic protein within the PGS-*co*-PEG nanoparticles, we selected fluorescein isothiocyanate-labeled bovine serum albumin (FITC-BSA) as a model protein. FITC-BSA was encapsulated within nanoparticles using the nanoprecipitation method. The encapsulation efficiency of these nanoparticles was 88.5% and 91% for PGS-20PEG and PGS-40PEG, respectively. The TEM and DLS data indicated an increase in the size of nanoparticles with an increase in protein loading (Fig. 2a & 2b). The addition of 25, 50, and 100 μ g of FITC-BSA to PGS-20PEG increased the nanoparticle size from ~ 270 nm to 350, 610, and 840 nm, respectively. A similar trend was observed in

PGS-40PEG. These findings indicate that the size of nanoparticles can be controlled by altering the protein loading. Although large-size nanoparticles (>500 nm), cannot be used for therapeutic delivery *via* systemic injection, but they have potential to be incorporated within tissue engineering scaffold to provide biochemical cues. By sustained release of therapeutic within bioengineered scaffolds, cell migration and fate can be controlled. The increase in nanoparticle size due to protein loading might be attributed to localization of protein within hydrophobic domain (PGS) of nanoparticles. Similar results have been reported earlier with spherical nanoparticles.¹⁵

3.4 Hemo- and immune-compatibility of Ellipsoidal Nanoparticles

The surface characteristics of nanoparticles determine hemo- and immune-compatibility of nanoparticles. Proteins get adsorbed on nanoparticles surface as soon as it comes in contact with biological fluids resulting in formation of protein corona. The type and amount of protein adsorbed on nanoparticles surface determine biological fate, therapeutic efficiency and toxicity of nanoparticles. The size of protein corona on PGS-PEG nanoparticles directly depend on the density and length of PEG block. It is expected that both PGS-20PEG and PGS-40PEG nanoparticles will have high hemo- and immune- compatibility due to presence of PEG on the surface. It is also expected that PGS-40PEG have higher PEG density on surface compared to PGS-20PEG nanoparticles, thus should show superior hemo- and immune- compatibility.

For systemic administration for targeted and controlled drug delivery, the mechanism of interaction of nanoparticles with blood needs to be investigated. *In vivo* circulation time directly depend on nanoparticle stability in physiological conditions.⁵¹ We investigated the hemocompatibility of nanoparticles by determining the release of hemoglobin from red blood cells (erythrocytes) and whole blood after exposure to PGS-PEG nanoparticles (Fig. 3a). Purified bovine red blood cells (erythrocytes) were obtained by separating plasma proteins from whole blood and were subjected to different concentration of nanoparticles to investigate hemolysis ability of nanoparticles. After 24 h of incubating the nanoparticles with red blood cells and whole blood, the supernatant was used to quantify hemolysis. PGS-20PEG nanoparticles showed no hemolysis at a low concentration (<1 µg/mL). However, at higher PGS-20PEG nanoparticle concentrations (5 µg/mL and 10 µg/mL), 5–10% hemolysis was observed. Interestingly, when the same experiment was performed with PGS-40PEG nanoparticles, we observed less than 2% hemolysis after 3 h of incubation, even for the highest nanoparticle concentration. While no hemolysis was observed in whole blood in both type of nanoparticles. This might be due to presence of serum protein that might prevent any hemolysis in whole blood. Our findings indicate that an increase in PEG concentration increases the hemocompatibility of the nanoparticles. These results are in accordance with the literature supporting the ability of PEGylation to enhance hemocompatibility of nanoparticles.^{52,53}

Polymeric nanoparticles with long-circulating time are able to improve the clinical efficacy of therapeutic delivery by improving pharmacokinetics, drug localization and delivery efficacy.^{54,55} Nanoparticles with stealth capability are able to have long circulating time, as they are able to maintain their structural stability without elicit an immune response.^{56,57}

The stealth capability of PGS-co-PEG nanoparticles is expected to improve the immunocompatibility of nanoparticles. We evaluated the immunocompatibility of nanoparticles by monitoring the expression level of two co-stimulatory molecules-CD80 and CD86 of macrophages *in vitro*. Incubation with increasing doses of PGS-co-PEG nanoparticles did not induce any upregulation of co-stimulatory surface markers on macrophages (Fig. 3b). In contrast, lipopolysaccharide, a potent immunostimulatory component of bacterial membrane, induced a significant increase in CD80 and CD86 surface expression on macrophages. This highlights the high immunocompatibility of PGS-co-PEG nanoparticles.

3.5 In vitro Cytocompatibility of Ellipsoidal Nanoparticles

The *in vitro* compatibility of PGS-co-PEG nanoparticles was investigated using preosteoblast cells (MC3T3). Cellular viability, proliferation, and morphology were evaluated at different nanoparticle concentrations. The effect of nanoparticles on cellular morphology was monitored by staining the cells for actin cytoskeleton and nucleus after 3 h and 24 h incubation (Fig. 4a). The untreated cells were flat and adherent to the substrate, with well-defined cytoskeletal structures and strong peripheral F-actin along the cell edges indicating cortical actin fibers. No significant difference was observed in cellular morphology when treated with 0.1 mg/mL and 1 mg/mL of PGS-20PEG (and PGS-40PEG) nanoparticles. However, at a higher concentration (10 mg/mL), cell shrinkage was observed due to the disruption of the actin cytoskeleton. For PGS-40PEG nanoparticles, higher concentrations of nanoparticles resulted in cells clustering with no clear sign of actin, confirming disorganization of the cytoskeleton. After 24 h, the actin cytoskeleton showed distinct morphological features caused by prolonged incubation time, which possibly obscured the actin filaments (F-actin). Earlier studies have also showed that disruption of cytoskeleton indicates potential toxicity of nanoparticles.^{58,59}

The quantitative cytotoxicity of these ellipsoidal nanoparticles was evaluated by monitoring mitochondrial activity, which affects cell viability and metabolic activity through MTS assay. The results showed that the metabolic activity of the cells did not change after 3 h or 24 h at lower concentrations by either of the compositions. For example, at low nanoparticle concentration (<1 mg/mL), no significant change in cellular viability was observed. However, at a higher nanoparticle concentration (>1 mg/mL), a sudden decrease in cellular viability was observed. The half maximal inhibitory concentration (IC₅₀) for PGS-co-PEG nanoparticles was determined by fitting the dose response curve to the experimental data. The IC₅₀ for PGS-20PEG and PGS-40PEG was obtained around 6.3 mg/mL after 24 h exposure. The IC₅₀ of PGS-20PEG and PGS-40PEG nanoparticles were similar to other types of nanoparticles such as PLGA and PLGA-co-PEG nanoparticles.^{42,44,60,61}

3.6 Intracellular Delivery via Nanoparticles

To further investigate cellular effects of nanoparticles, the internalization of nanoparticles on the endocytosis pathways of preosteoblast and endothelial cells was determined using flow cytometry. Specifically, three different endocytosis pathways— micropinocytosis, calveolae-mediated and clathrin-mediated—were blocked using their respective inhibitor drugs wortmannin, nystatin, and chlorpromazine.^{62–64} Cells were treated with empty

nanoparticles, and FITC-BSA loaded PGS-20PEG nanoparticles in presence of different inhibitory drugs and compared with untreated cells. There was no significant difference between empty nanoparticles and untreated cells, this was due to absence of FITC-BSA in nanoparticles. The results showed that wortmannin and chlorpromazine showed significant suppression of cellular uptake of nanoparticles as compared to the control (no drug), indicating that micropinocytosis and clathrin-mediated endocytosis pathways are predominately responsible for nanoparticles uptake (Fig. 5). The mean fluorescence intensity of cells treated with and without nanoparticles indicated a higher uptake of nanoparticles by preosteoblasts compared to endothelial cells.

4. Conclusions

We introduce a novel yet effective mode of synthesis of a self-assembled ellipsoidal nanoparticle system consisting of an amphiphilic copolymer derived from poly (glycerol sebacate) and poly(ethylene glycol) for therapeutic delivery. The proposed PGS-*co*-PEG nanoparticle system is highly tunable, and the semi-axis length of the nanoparticle can be modulated by therapeutic loading. PGS-*co*-PEG nanoparticles showed high cyto-, immune- and hemo- compatibility. Furthermore, the results of this study indicate that ellipsoidal nanoparticles could have a wide range of highly promising applications for proteins and peptide delivery which is claimed to be one of the rapidly developing key components in modern medical breakthrough such as regenerative medicine, stem cell engineering, immune modulation, and cancer therapeutics.

Acknowledgments

A.K.G would like to acknowledge funding support from National Institute of Health (EB026265), Texas Engineering Experiment Station, Texas A&M University Seed Grant. R.S.S was supported by the Cornell University Engineering Learning Initiative grant. A.S. would like to acknowledge funding support from Cornell University's Sibley School of Mechanical and Aerospace Engineering and College of Engineering.

References

1. Mura S, Nicolas J, Couvreur P. Stimuli-responsive nanocarriers for drug delivery. *Nature materials*. 2013; 12(11):991–1003. [PubMed: 24150417]
2. Petros RA, DeSimone JM. Strategies in the design of nanoparticles for therapeutic applications. *Nature Reviews Drug Discovery*. 2010; 9(8):615–627. [PubMed: 20616808]
3. Dobrovolskaia MA, McNeil SE. Immunological properties of engineered nanomaterials. *Nature nanotechnology*. 2007; 2(8):469–478.
4. Kamaly N, Yameen B, Wu J, Farokhzad OC. Degradable controlled-release polymers and polymeric nanoparticles: mechanisms of controlling drug release. *Chemical reviews*. 2016; 116(4):2602–2663. [PubMed: 26854975]
5. Panyam J, Labhasetwar V. Biodegradable nanoparticles for drug and gene delivery to cells and tissue. *Advanced drug delivery reviews*. 2003; 55(3):329–347. [PubMed: 12628320]
6. Kerativitayanan P, Carrow JK, Gaharwar AK. Nanomaterials for Engineering Stem Cell Responses. *Advanced Healthcare Materials*. 2015; 4(11):1600–1627. [PubMed: 26010739]
7. Tonga GY, Saha K, Rotello VM. 25th anniversary article: interfacing nanoparticles and biology: new strategies for biomedicine. *Advanced Materials*. 2014; 26(3):359–370. [PubMed: 24105763]
8. Sun T, Zhang YS, Pang B, Hyun DC, Yang M, Xia Y. Engineered nanoparticles for drug delivery in cancer therapy. *Angewandte Chemie International Edition*. 2014; 53(46):12320–12364. [PubMed: 25294565]

9. Torchilin VP. Multifunctional, stimuli-sensitive nanoparticulate systems for drug delivery. *Nature reviews Drug discovery*. 2014; 13(11):813–827. [PubMed: 25287120]
10. Singh A, Agarwal R, Diaz-Ruiz CA, Willett NJ, Wang P, Lee LA, Wang Q, Guldberg RE, García AJ. Nanoengineered Particles for Enhanced Intra-Articular Retention and Delivery of Proteins. *Advanced healthcare materials*. 2014; 3(10):1562–1567. [PubMed: 24687997]
11. Chithrani BD, Ghazani AA, Chan WC. Determining the size and shape dependence of gold nanoparticle uptake into mammalian cells. *Nano letters*. 2006; 6(4):662–668. [PubMed: 16608261]
12. He C, Hu Y, Yin L, Tang C, Yin C. Effects of particle size and surface charge on cellular uptake and biodistribution of polymeric nanoparticles. *Biomaterials*. 2010; 31(13):3657–3666. [PubMed: 20138662]
13. Mu Q, Su G, Li L, Gilbertson BO, Yu LH, Zhang Q, Sun Y-P, Yan B. Size-dependent cell uptake of protein-coated graphene oxide nanosheets. *ACS applied materials & interfaces*. 2012; 4(4):2259–2266. [PubMed: 22409495]
14. Jin H, Heller DA, Sharma R, Strano MS. Size-dependent cellular uptake and expulsion of single-walled carbon nanotubes: single particle tracking and a generic uptake model for nanoparticles. *Acs Nano*. 2009; 3(1):149–158. [PubMed: 19206261]
15. Whitmire RE, Scott Wilson D, Singh A, Levenston ME, Murthy N, García AJ. Self-assembling nanoparticles for intra-articular delivery of anti-inflammatory proteins. *Biomaterials*. 2012
16. Albanese A, Tang PS, Chan WC. The effect of nanoparticle size, shape, and surface chemistry on biological systems. *Annual review of biomedical engineering*. 2012; 14:1–16.
17. Verma A, Stellacci F. Effect of surface properties on nanoparticle–cell interactions. *Small*. 2010; 6(1):12–21. [PubMed: 19844908]
18. Dasgupta S, Auth T, Gompper G. Shape and orientation matter for the cellular uptake of nonspherical particles. *Nano letters*. 2014; 14(2):687–693. [PubMed: 24383757]
19. Williford J-M, Santos JL, Shyam R, Mao H-Q. Shape control in engineering of polymeric nanoparticles for therapeutic delivery. *Biomaterials Science*. 2015
20. Chimene D, Alge DL, Gaharwar AK. Two-Dimensional Nanomaterials for Biomedical Applications: Emerging Trends and Future Prospects. *Adv Mater*. 2015; 27(45):7261–84. [PubMed: 26459239]
21. Blanco E, Shen H, Ferrari M. Principles of nanoparticle design for overcoming biological barriers to drug delivery. *Nature biotechnology*. 2015; 33(9):941–951.
22. Meyer RA, Sunshine JC, Perica K, Kosmides AK, Aje K, Schneck JP, Green JJ. Biodegradable Nanoellipsoidal Artificial Antigen Presenting Cells for Antigen Specific T-Cell Activation. *Small*. 2015; 11(13):1519–1525. [PubMed: 25641795]
23. Gratton SEA, Ropp PA, Pohlhaus PD, Luft JC, Madden VJ, Napier ME, DeSimone JM. The effect of particle design on cellular internalization pathways. *Proceedings of the National Academy of Sciences*. 2008; 105(33):11613–11618.
24. Florez L, Herrmann C, Cramer JM, Hauser CP, Koynov K, Landfester K, Crespy D, Mailänder V. How Shape Influences Uptake: Interactions of Anisotropic Polymer Nanoparticles and Human Mesenchymal Stem Cells. *Small*. 2012; 8(14):2222–2230. [PubMed: 22528663]
25. Zhang Y, Nayak TR, Hongb H, Cai W. Graphene: a versatile nanoplatform for biomedical applications. *Nanoscale*. 2012; 4:3833. [PubMed: 22653227]
26. Agarwal R, Singh V, Journey P, Shi L, Sreenivasan SV, Roy K. Mammalian cells preferentially internalize hydrogel nanodiscs over nanorods and use shape-specific uptake mechanisms. *PNAS*. 2013; 110(43):17247–17252. [PubMed: 24101456]
27. Zhang Y, Tekobo S, Tu Y, Zhou Q, Jin X, Dergunov SA, Pinkhassik E, Yan B. Permission to Enter Cell by Shape: Nanodisk vs Nanosphere. *ACS Appl. Mater. Inter*. 2012; 4:4099–4105.
28. Glotzer SC, Solomon MJ. Anisotropy of building blocks and their assembly into complex structures. *Nature materials*. 2007; 6(8):557–562. [PubMed: 17667968]
29. Hickey JW, Santos JL, Williford J-M, Mao H-Q. Control of polymeric nanoparticle size to improve therapeutic delivery. *Journal of Controlled Release*. 2015; 219:536–547. [PubMed: 26450667]
30. Grzelczak M, Vermant J, Furst EM, Liz-Marzán LM. Directed Self-Assembly of Nanoparticles. *ACS Nano*. 2010; 4(7):3591–3605. [PubMed: 20568710]

31. Merkel TJ, Herlihy KP, Nunes J, Orgel RM, Rolland JP, DeSimone JM. Scalable, Shape-Specific, Top-Down Fabrication Methods for the Synthesis of Engineered Colloidal Particles. *Langmuir*. 2010; 26(16):13086–13096. [PubMed: 20000620]
32. Wang Y, Kim YM, Langer R. In vivo degradation characteristics of poly(glycerol sebacate). *Journal of Biomedical Materials Research Part A*. 2003; 66A(1):192–197.
33. Wang YD, Ameer GA, Sheppard BJ, Langer R. A tough biodegradable elastomer. *Nature Biotechnology*. 2002; 20(6):602–606.
34. Loh XJ, Karim AA, Owh C. Poly (glycerol sebacate) biomaterial: synthesis and biomedical applications. *Journal of Materials Chemistry B*. 2015; 3(39):7641–7652.
35. Rai R, Tallawi M, Grigore A, Boccaccini AR. Synthesis, properties and biomedical applications of poly(glycerol sebacate) (PGS): A review. *Progress in Polymer Science*. 2012; 37:1051–1078.
36. Monopoli MP, Aberg C, Salvati A, Dawson KA. Biomolecular coronas provide the biological identity of nanosized materials. *Nat Nano*. 2012; 7(12):779–786.
37. Otsuka H, Nagasaki Y, Kataoka K. PEGylated nanoparticles for biological and pharmaceutical applications. *Advanced drug delivery reviews*. 2003; 55(3):403–419. [PubMed: 12628324]
38. Suk JS, Xu Q, Kim N, Hanes J, Ensign LM. PEGylation as a strategy for improving nanoparticle-based drug and gene delivery. *Advanced drug delivery reviews*. 2016; 99:28–51. [PubMed: 26456916]
39. Jokerst JV, Lobovkina T, Zare RN, Gambhir SS. Nanoparticle PEGylation for imaging and therapy. *Nanomedicine*. 2011; 6(4):715–728. [PubMed: 21718180]
40. Patel A, Gaharwar AK, Iviglia G, Zhang H, Mukundan S, Mihaila SM, Demarchi D, Khademhosseini A. Highly elastomeric poly (glycerol sebacate)-co-poly (ethylene glycol) amphiphilic block copolymers. *Biomaterials*. 2013; 34(16):3970–3983. [PubMed: 23453201]
41. Bilati U, Allémann E, Doelker E. Development of a nanoprecipitation method intended for the entrapment of hydrophilic drugs into nanoparticles. *European Journal of Pharmaceutical Sciences*. 2005; 24(1):67–75. [PubMed: 15626579]
42. Govender T, Stolnik S, Garnett MC, Illum L, Davis SS. PLGA nanoparticles prepared by nanoprecipitation: drug loading and release studies of a water soluble drug. *Journal of Controlled Release*. 1999; 57(2):171–185. [PubMed: 9971898]
43. Dobrovolskaia MA, Clogston JD, Neun BW, Hall JB, Patri AK, McNeil SE. Method for analysis of nanoparticle hemolytic properties in vitro. *Nano letters*. 2008; 8(8):2180–2187. [PubMed: 18605701]
44. Cheng J, Teply BA, Sherifi I, Sung J, Luther G, Gu FX, Levy-Nissenbaum E, Radovic-Moreno AF, Langer R, Farokhzad OC. Formulation of functionalized PLGA–PEG nanoparticles for in vivo targeted drug delivery. *Biomaterials*. 2007; 28(5):869–876. [PubMed: 17055572]
45. Riley T, Govender T, Stolnik S, Xiong C, Garnett M, Illum L, Davis S. Colloidal stability and drug incorporation aspects of micellar-like PLA–PEG nanoparticles. *Colloids and surfaces B: Biointerfaces*. 1999; 16(1):147–159.
46. Zhang Y, Zhuo R-x. Synthesis and in vitro drug release behavior of amphiphilic triblock copolymer nanoparticles based on poly (ethylene glycol) and polycaprolactone. *Biomaterials*. 2005; 26(33): 6736–6742. [PubMed: 15935469]
47. Gref R, Lück M, Quellec P, Marchand M, Dellacherie E, Harnisch S, Blunk T, Müller R. ‘Stealth’ corona-core nanoparticles surface modified by polyethylene glycol (PEG): influences of the corona (PEG chain length and surface density) and of the core composition on phagocytic uptake and plasma protein adsorption. *Colloids and Surfaces B: Biointerfaces*. 2000; 18(3):301–313. [PubMed: 10915952]
48. Surnar B, Sharma K, Jayakannan M. Core–shell polymer nanoparticles for prevention of GSH drug detoxification and cisplatin delivery to breast cancer cells. *Nanoscale*. 2015; 7(42):17964–17979. [PubMed: 26465291]
49. Jiang W, Kim BY, Rutka JT, Chan WC. Nanoparticle-mediated cellular response is size-dependent. *Nature nanotechnology*. 2008; 3(3):145–150.
50. Walkey CD, Olsen JB, Guo H, Emili A, Chan WC. Nanoparticle size and surface chemistry determine serum protein adsorption and macrophage uptake. *Journal of the American Chemical Society*. 2012; 134(4):2139–2147. [PubMed: 22191645]

51. Nel AE, Mädler L, Velegol D, Xia T, Hoek EM, Somasundaran P, Klaessig F, Castranova V, Thompson M. Understanding biophysicochemical interactions at the nano–bio interface. *Nature materials*. 2009; 8(7):543–557. [PubMed: 19525947]
52. Kuo W-H, Wang M-J, Chang C-W, Wei T-C, Lai J-Y, Tsai W-B, Lee C. Improvement of hemocompatibility on materials by photoimmobilization of poly (ethylene glycol). *Journal of Materials Chemistry*. 2012; 22(19):9991–9999.
53. Wang W, Xiong W, Zhu Y, Xu H, Yang X. Protective effect of PEGylation against poly (amidoamine) dendrimer-induced hemolysis of human red blood cells. *Journal of Biomedical Materials Research Part B: Applied Biomaterials*. 2010; 93(1):59–64.
54. Naahidi S, Jafari M, Edalat F, Raymond K, Khademhosseini A, Chen P. Biocompatibility of engineered nanoparticles for drug delivery. *Journal of controlled release*. 2013; 166(2):182–194. [PubMed: 23262199]
55. Hu C-MJ, Fang RH, Luk BT, Zhang L. Polymeric nanotherapeutics: clinical development and advances in stealth functionalization strategies. *Nanoscale*. 2014; 6(1):65–75. [PubMed: 24280870]
56. Moyano DF, Goldsmith M, Solfiell DJ, Landesman-Milo D, Miranda OR, Peer D, Rotello VM. Nanoparticle hydrophobicity dictates immune response. *Journal of the American Chemical Society*. 2012; 134(9):3965–3967. [PubMed: 22339432]
57. Zolnik BS, Gonzalez-Fernandez A, Sadrieh N, Dobrovolskaia MA. Minireview: nanoparticles and the immune system. *Endocrinology*. 2010; 151(2):458–465. [PubMed: 20016026]
58. Lewinski N, Colvin V, Drezek R. Cytotoxicity of nanoparticles. *small*. 2008; 4(1):26–49. [PubMed: 18165959]
59. Panariti A, Miserocchi G, Rivolta I. The effect of nanoparticle uptake on cellular behavior: disrupting or enabling functions? *Nanotechnology, science and applications*. 2012; 5:87.
60. Danhier F, Lecouturier N, Vroman B, Jérôme C, Marchand-Brynaert J, Feron O, Préat V. Paclitaxel-loaded PEGylated PLGA-based nanoparticles: in vitro and in vivo evaluation. *Journal of Controlled Release*. 2009; 133(1):11–17. [PubMed: 18950666]
61. Wang H, Zhao Y, Wu Y, Hu Y-l, Nan K, Nie G, Chen H. Enhanced anti-tumor efficacy by co-delivery of doxorubicin and paclitaxel with amphiphilic methoxy PEG-PLGA copolymer nanoparticles. *Biomaterials*. 2011; 32(32):8281–8290. [PubMed: 21807411]
62. Herd H, Daum N, Jones AT, Huwer H, Ghandehari H, Lehr C-M. Nanoparticle geometry and surface orientation influence mode of cellular uptake. *ACS nano*. 2013; 7(3):1961–1973. [PubMed: 23402533]
63. Greulich C, Diendorf J, Simon T, Eggeler G, Epple M, Köller M. Uptake and intracellular distribution of silver nanoparticles in human mesenchymal stem cells. *Acta biomaterialia*. 2011; 7(1):347–354. [PubMed: 20709196]
64. Sokolova V, Kozlova D, Knuschke T, Buer J, Westendorf AM, Epple M. Mechanism of the uptake of cationic and anionic calcium phosphate nanoparticles by cells. *Acta biomaterialia*. 2013; 9(7): 7527–7535. [PubMed: 23454056]

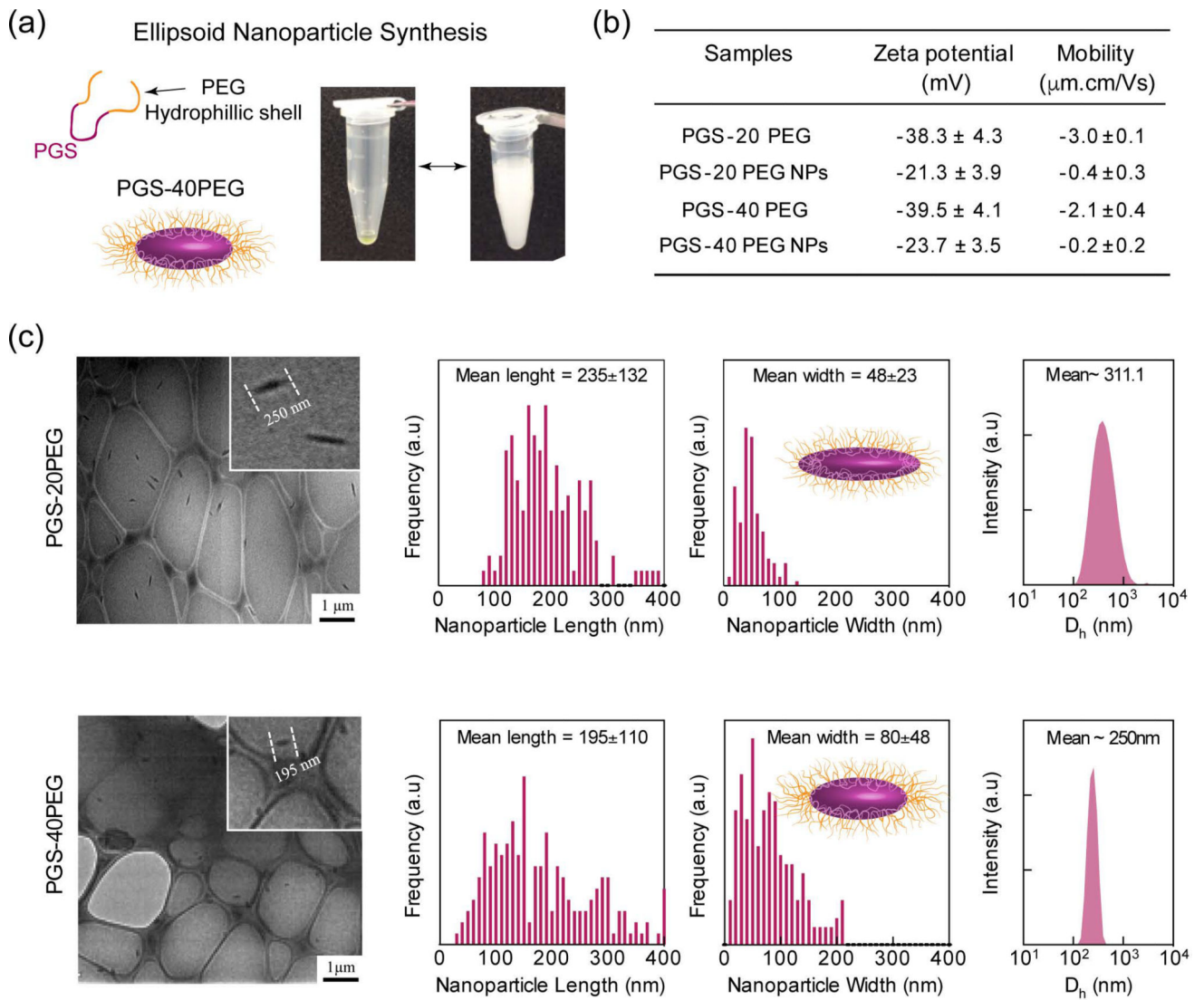


Figure 1.

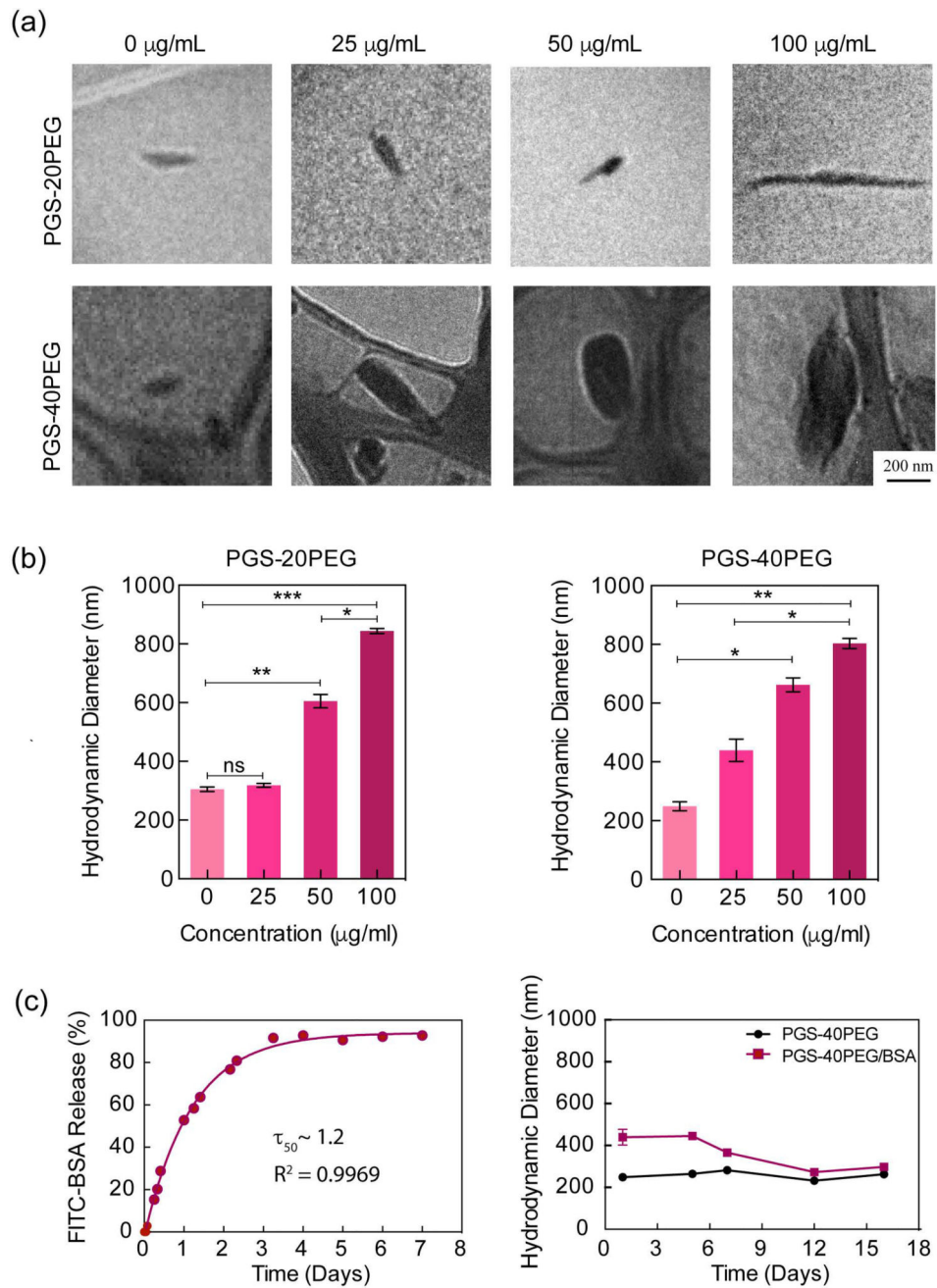


Figure 2.

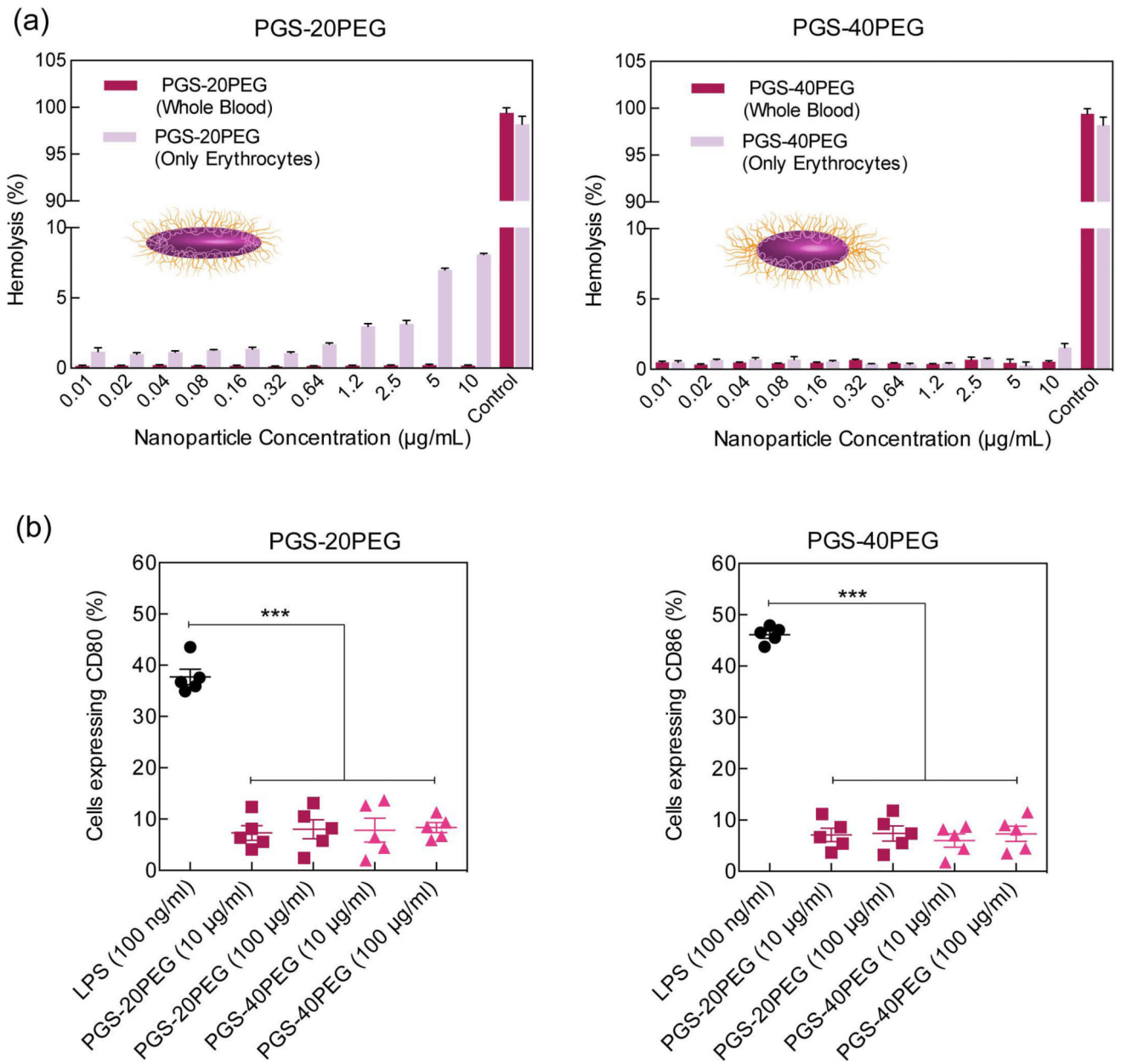
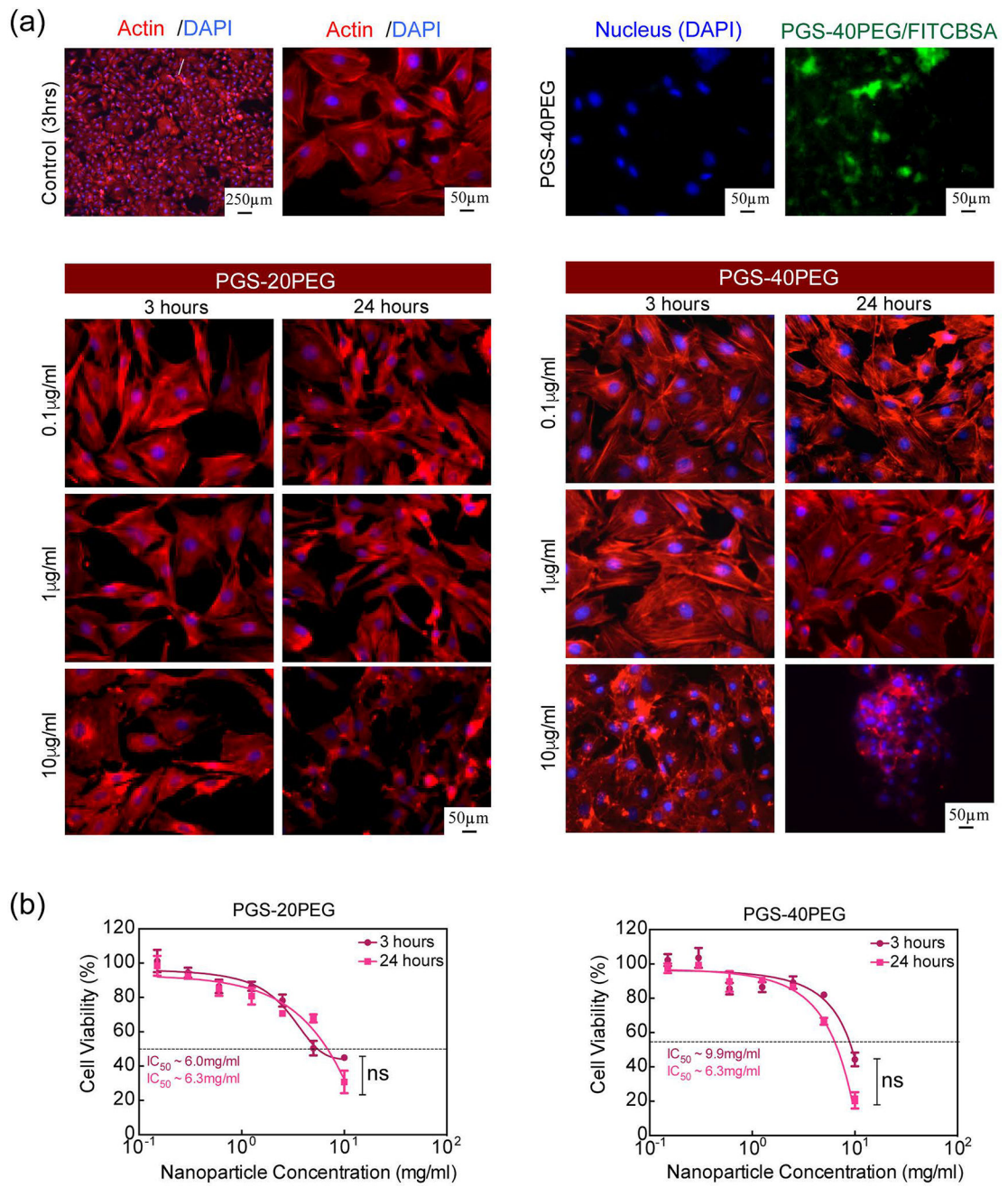


Figure 3.



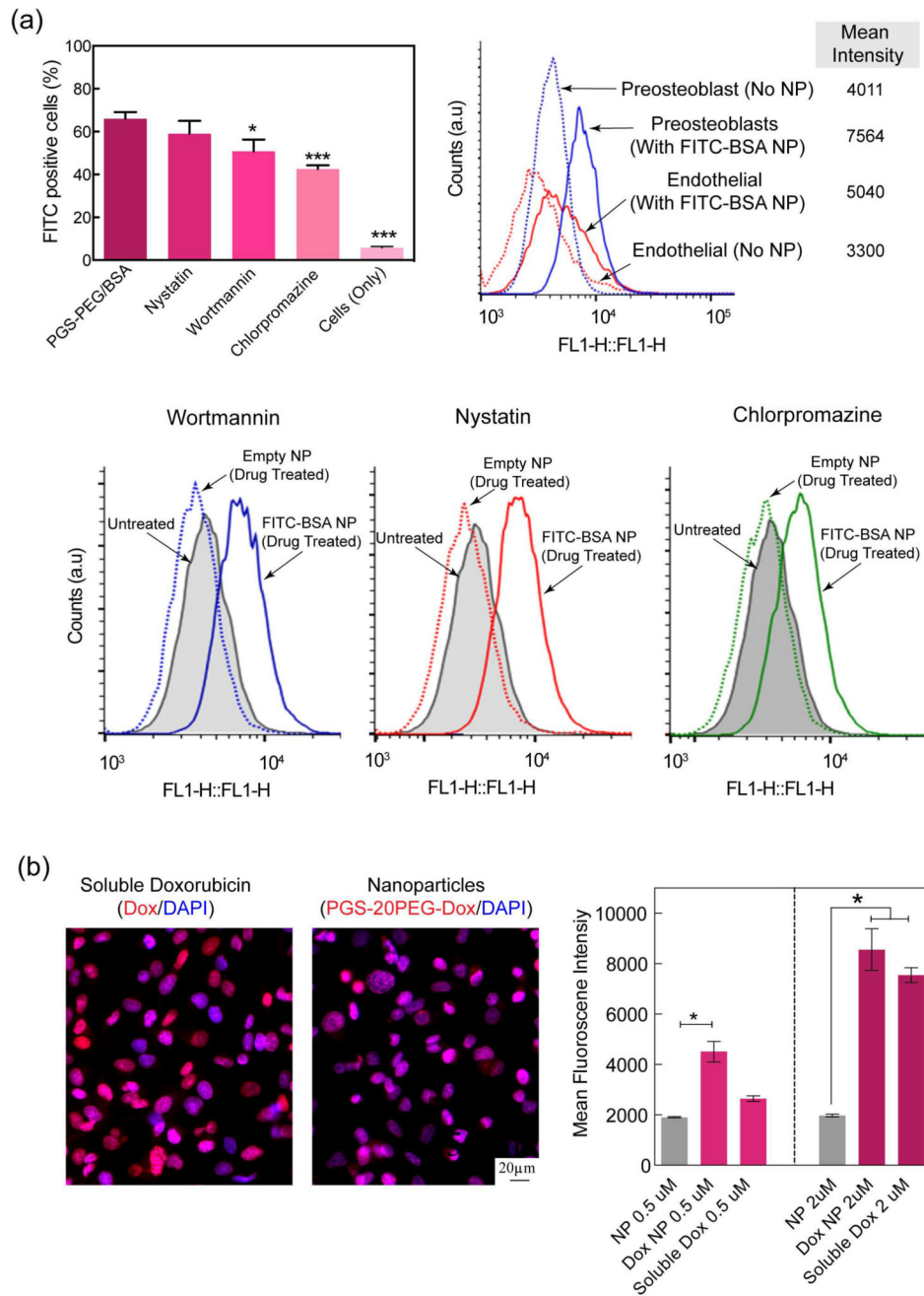


Figure 5.